JOC The Journal of Organic Chemistry

pubs.acs.org/joc Article

Targeting Intracellular Pathogenic Bacteria Through N-Terminal Modification of Cationic Amphiphilic Polyproline Helices

Thomas A. Dietsche, Hassan E. Eldesouky, Samantha M. Zeiders, Mohamed N. Seleem, and Jean Chmielewski*

Cite This: J. Org. Chem. 2020, 85, 7468–7475 Read Online

ACCESS | Metrics & More | Article Recommendations | Supporting Information

ABSTRACT: Intracellular pathogens can thrive within mammalian cells and are inaccessible to many antimicrobial agents. Herein, we present a facile method of enhancing the cell penetrating and antibacterial properties of cationic amphiphilic polyproline helices (CAPHs) with modifications to the hydrophobic moiety at the N-terminus. These altered CAPHs display superior cell penetration within macrophage cells, and in some cases, minimal cytotoxicity. Furthermore, one CAPH, **Pentyl-P14** exhibited excellent antibacterial activity against multiple strains of pathogenic bacteria and promoted the clearance of intracellular *Shigella* within macrophages.

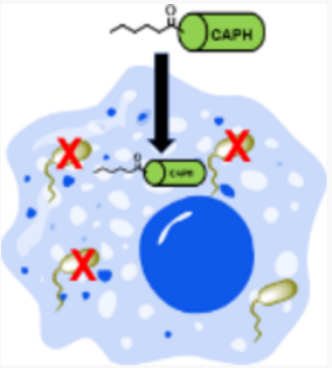

INTRODUCTION

The rise of antimicrobial resistance has created a global health crisis whereby many antibiotics have become ineffective. A number of antibiotic-resistant strains, including the multidrug-resistant *Acinetobacter baumannii* (*A. baumannii*), remain difficult to treat.[1,2] This problem is further compounded by the issue that many bacteria such as *Listeria monocytogenes* (*L. monocytogenes*), *Mycobacterium tuberculosis* (*M. tuberculosis*), and *Shigella flexneri* (*S. flexneri*) can invade mammalian cells.[3,4] Once inside the cell, these bacteria evade host immune responses and many therapeutics that do not accumulate sufficiently within cells.[5,6] To combat this challenge, new antibiotics are needed that can effectively penetrate mammalian cells and eliminate these pathogenic bacteria.

Delivery systems targeting intracellular pathogens have been developed, such as nanoparticles containing antibiotics.[7,8] An alternative approach has been to use cell-penetrating peptides in conjugation with antibiotics and peptide nucleic acids.[9−11] Cell-penetrating peptides with inherent antibacterial properties have also been developed.[12,13] These synthetic peptides were composed of a cationic amphiphilic polyproline helix (CAPH) scaffold and contained both hydrophobic and cationic groups to imbue the molecule with amphiphilicity (Figure 1A). One such CAPH, **P14LRR**, has displayed promising cell penetration, broad-spectrum antibacterial activity, and modest reduction of bacteria within macrophage cells.[14]

In efforts to facilitate greater cell penetration, peptides have previously been modified with various aliphatic fatty acid moieties at the N-terminus to generate lipopeptides. Although these lipopeptides demonstrated an improvement in cell uptake, they suffered from extensive cytotoxicity.[15] While long aliphatic fatty acids may be impractical for potential therapeutics, it is possible that other hydrophobic moieties at the N-terminus could improve the cell penetration of CAPHs, while remaining noncytotoxic. Herein, we present our efforts to develop potent CAPHs with N-terminal hydrophobic modifications that could easily be adapted to other peptides to improve cell penetration and antimicrobial activity, while remaining nontoxic to cells. Furthermore, we demonstrate that these modifications on CAPHs can be utilized to clear intracellular pathogens *in cyto*.

RESULTS AND DISCUSSION

Altering the CAPH hydrophobic face has resulted in enhanced targeting of intracellular bacteria.[16] Therefore, we wished to evaluate the role of N-terminal hydrophobic moieties on cell penetration and antimicrobial activity (Figure 1B). To this end, five different functionalities at the N-terminus of CAPHs were designed: acetyl and pentyl aliphatic groups, and phenyl, naphthyl, and quinolyl aromatic groups (Figure 1B). These functionalities could easily be introduced on the N-terminus of resin-bound peptides. A 4-methyltrityl (Mtt)-protected lysine

Received: April 8, 2020
Published: May 19, 2020

https://dx.doi.org/10.1021/acs.joc.0c00871
J. Org. Chem. 2020, 85, 7468–7475

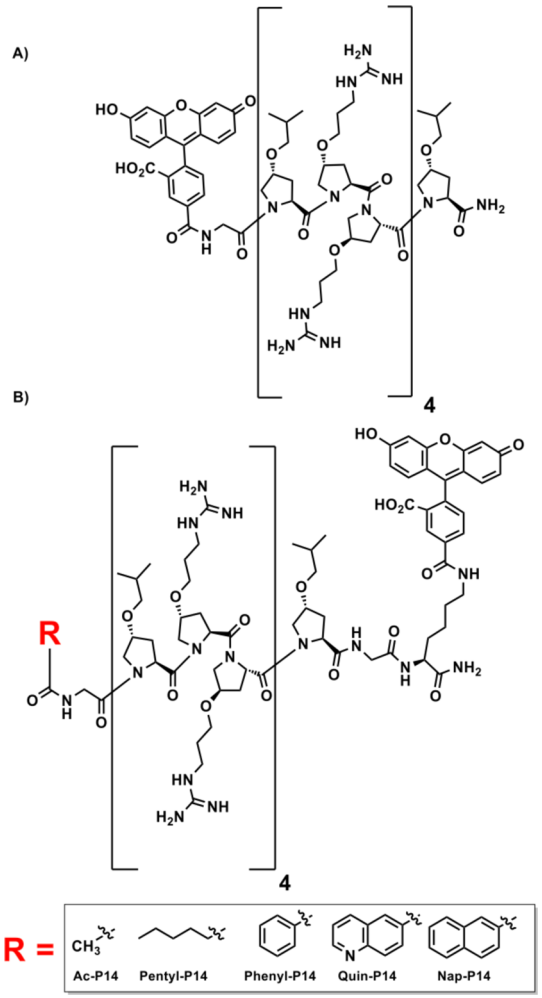

Figure 1. CAPHs. (A) Structure of **P14LRR** and (B) structure of CAPHs modified at the amino terminus with hydrophobic groups.

introduced at the carboxyl terminus of the peptide could be selectively deprotected and labeled with fluorescein for intracellular tracking. A glycine spacer between the (Mtt)-lysine residue was introduced to prevent unfavorable steric interactions with fluorescein.

The proline-modified unnatural amino acid containing the hydrophobic ($\mathbf{P_L}$) functionality was synthesized as previously described.[17] The guanidine-containing cationic $\mathbf{P_R}$ amino acid was synthesized following an improved three-step procedure (Scheme 1, top) as compared to the previously reported synthesis.[17] Briefly, amino acid analogue **2** was prepared by treating Cbz-hydroxyproline **1** with sodium hydride, followed by acrylonitrile. The Cbz protecting group of **2** was removed through hydrogenation and replaced with an Fmoc protecting group to provide analogue **3**. Finally, reduction of the nitrile group of **3**, followed by addition of *N*,*N*′-bis-Boc-1-guanylpyrazole yielded $\mathbf{P_R}$. This new synthetic strategy doubles the overall yield of the final product from 25 to 50% compared to the previously reported synthesis.[17]

The CAPH peptides were synthesized on a Rink amide resin using the standard Fmoc-based solid-phase peptide synthesis (SPPS) (Scheme 1, bottom). Following successful coupling at the N-terminus with the hydrophobic modifications, the (Mtt)-lysine was deprotected with hexafluoro-2-propanol (HFIP), and the resulting free amine was reacted with *N*-hydroxysuccinimide fluorescein. The peptides were cleaved from resin with concomitant side chain deprotection using a trifluoroacetic acid (TFA) cocktail. All peptides were purified to homogeneity by reverse-phase high-performance liquid chromatography (RP-HPLC) and characterized by matrix-assisted laser desorption ionization (MALDI) mass spectrometry.

Circular dichroism (CD) was used to evaluate the conformation of the newly synthesized CAPHs as it has previously been reported that modifications to polyproline type II (PPII) helices can affect conformational stability.[18] All CAPHs displayed a positive ellipticity at 225 nm that is

Scheme 1. Synthesis of $\mathbf{P_R}$ (Top) and On-Resin Coupling of Hydrophobic Functionalities on the N-Terminus of CAPH Peptides (Bottom)[a]

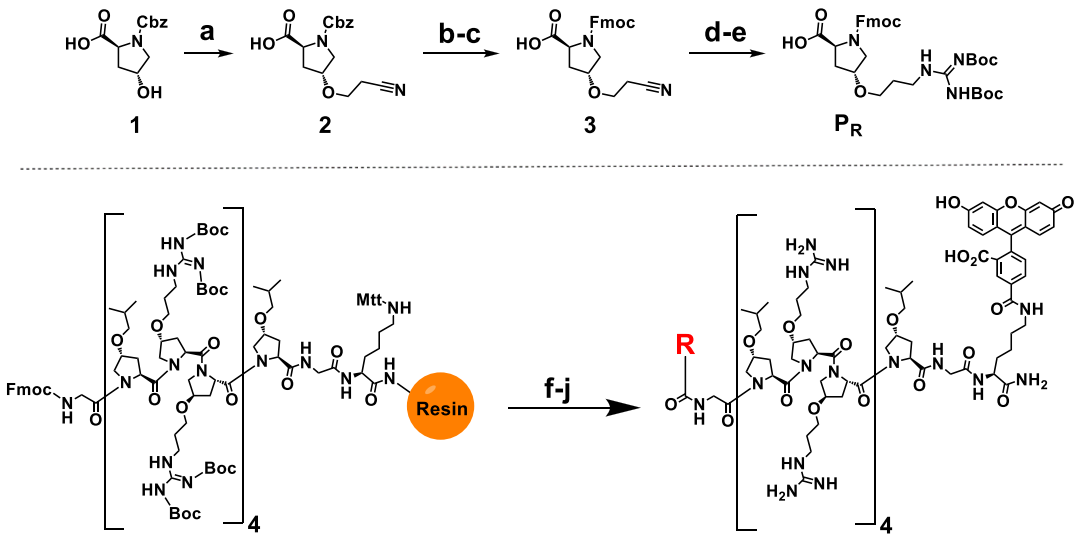

[a](a) Acrylonitrile, NaH, THF, 16 h, 80%. (b) H_2, Pd/C, MeOH. (c) Fmoc-OSu, $NaHCO_3$, acetone/H_2O, quant. (d) H_2, PtO_2, AcOH, MeOH, (e) *N*,*N*′-bis-Boc-1-guanylpyrazole, TEA, DCM, 62%, (f) piperidine (25% in DMF), 25 min. (g) R-CO_2H, DIEA, HATU, 3 h. (h) HFIP (30% in DCM), 2 × 30 min. (i) NHS-fluorescein, DIEA, DMF, 16 h. (j) 95% TFA, 2.5% TIPS, 2.5% H_2O, 2 h.

https://dx.doi.org/10.1021/acs.joc.0c00871
J. Org. Chem. 2020, 85, 7468−7475

characteristic of the PPII[19] (Figure S2), as was observed with the previous CAPHs.[17] These data support that the N-terminal modifications did not affect the secondary structure of the polyproline helix within CAPHs.

As many therapeutics suffer from the inability to effectively rescue mammalian cells from intracellular pathogens, it is imperative that antibacterial agents transverse the mammalian cell membrane. Thus, the N-terminal CAPHs were assessed for their ability to accumulate within J774A.1 macrophage cells using flow cytometry. Cells were incubated with each CAPH derivative, and the cellular fluorescence was measured in the presence of trypan blue (TB) to quench extracellular fluorescence that may be caused by a membrane-bound peptide.[20] Overall, the installation of various hydrophobic groups at the N-terminus drastically improved the ability of CAPHs to penetrate macrophage cells in comparison to **P14LRR** and the control peptide **Ac-P14** (Figure 2). Minor

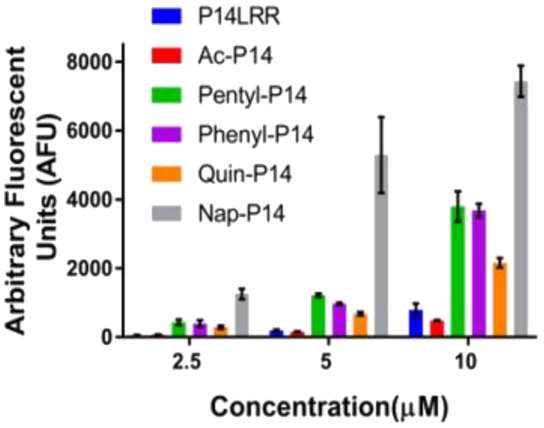

Figure 2. Cellular uptake of N-terminal CAPHs in J774A.1 macrophage cells. Cellular fluorescence was measured by flow cytometry after 1 h incubation with peptides. TB was used to quench fluorescence of membrane-bound peptides.

levels of membrane binding were observed for **Pentyl-P14**, **Phenyl-P14**, **Ac-P14**, and **Nap-P14**, as the decrease in cellular fluorescence with added TB was only 5−15% overall. In comparison, **Quin-P14** exhibited less-efficient cell penetration, as there was a decrease of up to 35% in cellular fluorescence when TB was added. At a concentration of 10 μM, **Phenyl-P14** and **Pentyl-P14** displayed about a fivefold increase in cell uptake compared to **P14LRR**, while **Quin-P14** displayed a more modest threefold increase. **Nap-P14** yielded the highest improvement compared to **P14LRR**, showing about an 11-fold higher cell uptake. Interestingly, **Nap-P14** displays almost four times the cell accumulation as **Quin-P14**, despite only differing by one nitrogen atom. Moreover, the CAPH derivative with the medium aliphatic chain, **Pentyl-P14**, was approximately eight times more efficient at cell penetration than **Ac-P14**, demonstrating that the length of the hydrophobic tail is crucial for cell penetration. These trends were consistent even at concentrations as low as 2.5 μM. Together, these results show that the N-terminal hydrophobic moiety can greatly impact the ability of CAPHs to penetrate mammalian cells.

Intracellular pathogens can take refuge in different subcellular locations such as vacuoles (*Mycobacterium*) and the cytosol (*L. monocytogenes* and *S. flexneri*), making treatment difficult. We had previously shown that altering the hydrophobic moieties on the backbone of CAPHs resulted in enhanced targeting of intracellular pathogens.[16] Similarly, we wished to investigate if the N-terminal modifications on CAPHs could affect their ability to localize to specific subcellular compartments. To this end, the subcellular localization of the N-terminal CAPHs was visualized via confocal microscopy. J774A.1 cells were incubated with CAPHs over a range of concentrations (2.5, 5, and 10 μM), and the cells were further treated with a Hoechst stain, Lysotracker, or Mitotracker to visualize the nucleus, endosomes, or mitochondria, respectively. At 5 μM, all CAPHs were found to localize primarily to the mitochondria with some cytosolic localization (Figure 3), whereas **Quin-P14** and **Nap-P14** also displayed nuclear localization in some cells (Figure S8). Interestingly, we observed concentration differences in the subcellular locations of these peptides. In all cases, with the exception of **Nap-14**, there was a threshold concentration at which the peptides switched from endosomal to mitochondrial localization; at 2.5 μM **Pentyl-P14**, **Phenyl-P14**, and **Quin-P14** were observed in both compartments, and for **Ac-P14,** this concentration was 5 μM (Figure S8). Below this concentration, the peptides were endosomal, and above this concentration, the peptides were localized to the mitochondria. This concentration dependence on subcellular location has been observed previously with **P14LRR**.[21] At all of the concentrations evaluated, Nap-P14 was found colocalized with Lysotracker and Mitotracker (Figure S8). These data demonstrate that the hydrophobic moieties at the N-terminus can direct CAPHs to the mitochondria and endosomes, with some cytosolic localization, and by fine-tuning the hydro-

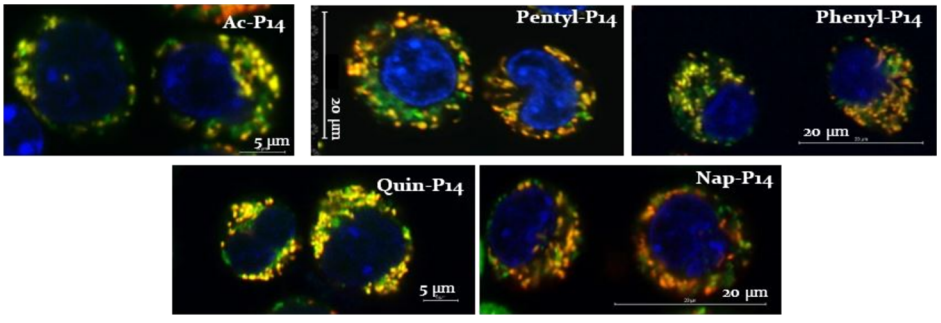

Figure 3. Subcellular localization of N-terminal CAPHs (green) in J774A.1 macrophage cells. Cells were treated with peptides (5 μM) (green) for 1 h. Following the incubation, cells were stained with Mitotracker (red) and Hoechst 3342 (blue) to visualize the mitochondria and nuclei, respectively. Cells were visualized by confocal microscopy, and the images show the overlay of the green, red, and blue channels for the treated cells.

https://dx.doi.org/10.1021/acs.joc.0c00871
J. Org. Chem. 2020, 85, 7468−7475

phobic group (bis-aromatic), CAPHs are found to localize in the nucleus as well.

To rescue macrophage cells from intracellular pathogens, mammalian cells must maintain their viability in the presence of antibiotic therapies. Thus, to ensure that the N-terminal modifications did not reduce cell viability below a reasonable level, CAPHs were screened against J774A.1 macrophage cells using the 3-(4,5-dimethylthiazol-2-yl)-2,5-diphenyltetrazolium bromide (MTT) assay at 10 μM for 9 h (Figure S3).[22] As mentioned earlier, long fatty acid N-terminal modifications have been shown to greatly improve cell penetration, but were toxic.[15] In contrast, four out of five of the N-terminally modified CAPHs displayed acceptable cell viability. **Ac-P14** and **P14LRR** displayed minimal toxicity in macrophage cells, whereas **Phenyl-P14**, **Pentyl-P14**, and **Quin-P14** showed acceptable cell viability (75−90%). **Nap-P14** displayed the lowest cell viability (60%), despite its improvement on cell penetration. From the cell uptake and cell viability data, it was determined that **Pentyl-P14** and **Phenyl-P14** satisfied two main requirements for application against intracellular pathogens: (1) efficient cell penetration and (2) limited toxicity in J774A.1 macrophage cells.

After determining that the N-terminal CAPHs boosted cell penetration, we investigated the antibacterial activity against a selection of Gram-positive and Gram-negative pathogens. An *in vitro* broth dilution assay was used to screen the potency of the CAPH derivatives against the intracellular bacteria *M. tuberculosis*, *L. monocytogenes,* and *S. flexneri*, *Escherichia Coli,* and the multidrug resistant *A. baumannii*.[11,23−25] **Quin-P14** was excluded because of the less-effective cell penetration, and **Nap-P14** was deemed to be too cytotoxic to continue forward. **Pentyl-P14** showed superior activity as compared to **Ac-P14** (Table 1), with two-fold increased potency against *M. tuberculosis*, *A. baumannii*, and *L. monocytogenes*, and four-fold enhanced potency against *E. coli* and *S. flexneri*. **Phenyl-P14** showed slightly lower activity against the before-mentioned pathogens as compared to **Pentyl-P14**. Although fluorophores were included within these peptides, we have previously shown that they play a minimal role in the antibiotic potency of CAPHs.[13]

Table 1. In Vitro Antibacterial Activity of CAPHs against Pathogenic Bacteria-MIC (μM)

	L. monocytogenes	*S. flexneri*	*M. tuberculosis*	*A. baumannii*	*E. coli*
P14LRR	8	8	16	16	4
Ac-P14	>16	16	16	16	8
Pentyl-P14	8	4	8	8	2
Phenyl-P14	16	8	16	8	4

A β-galactosidase release assay in *E. coli* was used to determine if the peptides acted through a cell lysis mechanism (Figure 4A). At 2× the minimum inhibitory concentration (MIC) values, **P14LRR** and **Pentyl-P14** showed minimal bacterial cell lysis, whereas the positive control mellitin displayed significant levels of lysis. **Ac-P14** and **Phenyl-P14** showed somewhat higher levels of lysis. At 4× the MIC values, the N-terminally modified CAPHs demonstrated lysis (Figure S4). This suggests that at higher peptide concentrations, membrane lysis could play a role in antibacterial activity.[26] However, there was no observed hemolysis with human red blood cells (hRBCs) up to 40 μM (Figure 4B), signifying that CAPHs may selectively lyse the bacterial membrane at higher concentrations, while leaving hRBCs intact.

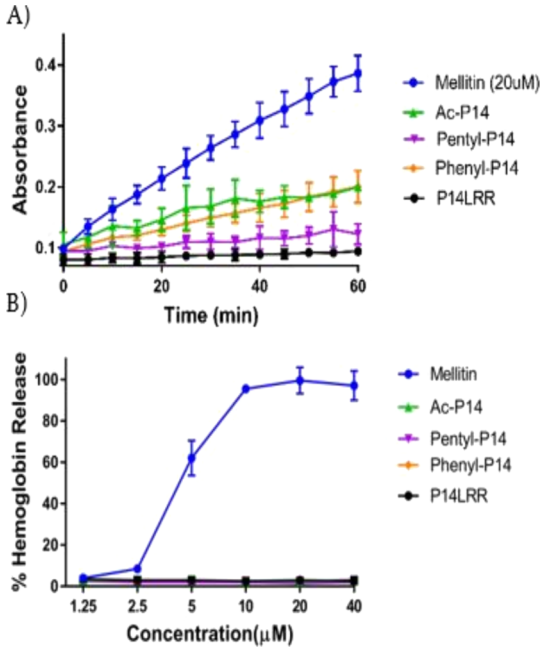

Figure 4. Investigating the mode of antimicrobial action of N-terminally modified CAPHs. (A) Leakage of β-galactosidase from *E. coli* after 1 h with CAPHs at 2× the MIC values. (B) Hemolysis of hRBCs when treated with CAPHs for 1 h.

With the confirmation that the N-terminally modified CAPHs possess both antibacterial activity and mammalian cell penetration, we probed clearance of the intracellular pathogen *S. flexneri* within J774A.1 macrophage cells.[27] **Pentyl-P14** was selected for this assay, as it exhibited the best combination of cell uptake, cell viability, and antimicrobial activity. **Ac-P14** was also evaluated, although it exhibited much lower cellular uptake and antibacterial activity. **Pentyl-P14** was found to clear ∼75% of *S. flexneri* within macrophage cells after 12 h, whereas **Ac-P14** exhibited a modest reduction (∼40%) of intracellular *S. flexneri* (Figure 5). These clearance results are likely due to a combination of several factors, including efficiency of cell penetration, antimicrobial activity, and

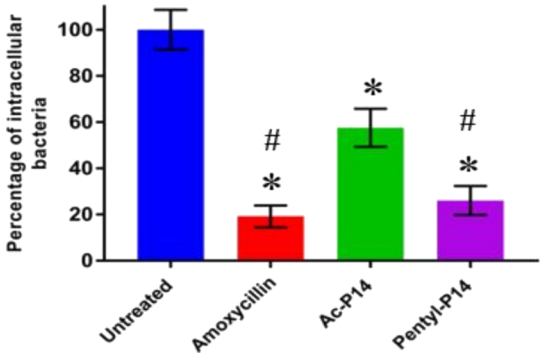

Figure 5. Intracellular bacterial clearance activity of **Pentyl-P14** and **Ac-P14** (10 μM) against *S. flexneri* in J774A.1 murine macrophage cells after 12 h. (*) denotes the statistical difference between the tested groups and the untreated control. (#) indicates a statistical significance with respect to **Ac-P14**. *#*P* values of <0.05 are considered significant.

https://dx.doi.org/10.1021/acs.joc.0c00871
J. Org. Chem. 2020, 85, 7468−7475

subcellular location. **Pentyl-P14** and **Ac-P14** were shown to localize mainly to the mitochondria with some cytosolic localization at 10 μM. Previous studies of CAPHs have shown a direct transport mechanism into the cytosol, followed by migration to the mitochondria.[28] While in the cytosol, **Pentyl-P14** is likely to interact with and eradicate *S. flexneri*, a cytoplasm-residing pathogen. Furthermore, **Pentyl-P14** possesses superior cell penetration and antibacterial activity against *S. flexneri* when compared to **Ac-P14**. Therefore, it stands to reason that **Pentyl-P14** would be more effective in clearing intracellular *S. flexneri*.

To further investigate if the pentyl moiety was an optimal N-terminal modification, four additional aliphatic modifications of CAPHs were synthesized containing C4−C7 tails: **Butyl-P14**, **Branched-P14**, **Hexyl-P14**, and **Heptyl-P14** (Figure 6).

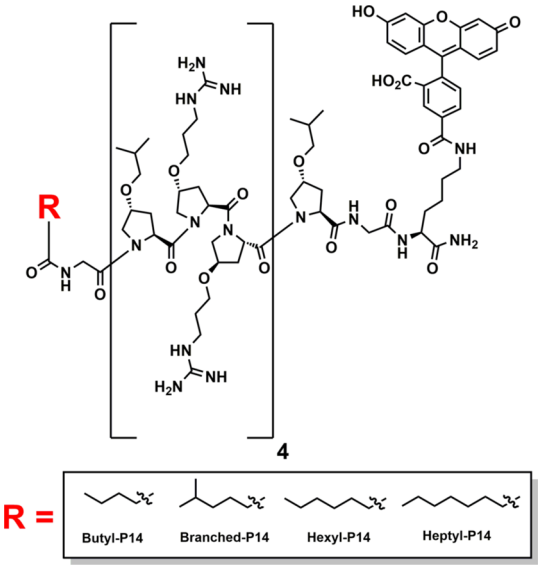

Figure 6. Structure of CAPHs modified at the amino terminus with additional aliphatic groups.

These CAPHs were assessed for their ability to penetrate mammalian cells via flow cytometry (Figure S6). At a concentration of 10 μM, **Butyl-P14** was about 10% less efficient at cell penetration as compared to **Pentyl-P14**. Conversely, **Branched-P14**, **Hexyl-P14**, and **Heptyl-P14** displayed increased cell accumulation at 10 μM as compared to **Pentyl-P14** (about four, two, and ninefold, respectively).

Unfortunately, the CAPHs that displayed superior cellular uptake as compared to **Pentyl-P14** also suffered from drastically reduced cell viability. **Branched-P14**, **Hexyl-P14**, and **Heptyl-P14** showed significant levels of toxicity, with cell viability ranging from 4 to 43% (Figure S7). The observation that longer N-terminal aliphatic chains result in severe cell toxicity is consistent with previous lipopeptide reports.[15] These data support the premise that the N-terminal pentyl modification represents the best compromise between cell accumulation and viability, as shorter aliphatic chains (**Ac-P14** and **Butyl-P14**) were not as efficacious in cell penetration. Conversely, longer aliphatic modifications (**Branched-P14**, **Hexyl-P14**, and **Heptyl-P14**) possessed greater cell penetration but were much more cytotoxic. Therefore, **Pentyl-P14** was deemed to be the most effective peptide, as it had excellent mammalian cell penetration while remaining noncytotoxic. We have previously observed an increase in cell toxicity with longer C6-aliphatic groups within the side chain functionalities of CAPHs.[16] Interestingly, this is also observed here with a single modification at the amino terminus.

CONCLUSIONS

In conclusion, combating intracellular bacteria remains a difficult challenge in the context of developing new therapeutics.[1−5] Functionalizing CAPHs with hydrophobic moieties at the N-terminus improved cell uptake and, in some cases, antibacterial activity. These N-terminal modifications are installed in a facile manner on a resin, making them easily adaptable to other peptides to improve their cell penetration or activity against intracellular pathogenic bacteria. By altering CAPHs to bear the five-carbon aliphatic chain, we found that **Pentyl-P14** was effective at clearing the intracellular pathogen *S. flexneri*. Therefore, **Pentyl-P14** is an excellent candidate to further the overarching goal of designing new therapeutics to target difficult-to-treat bacteria that reside within mammalian cells.

EXPERIMENTAL SECTION

Materials and Methods. Unless otherwise stated, common chemicals and solvents including Fmoc-protected amino acids, resins, carboxylic acids, and coupling reagents for SPPS were purchased from commercial sources and used without further purification. Compound **2** was purchased from Chem-Impex International. H-Rink Chem Matrix Rink amide resin (0.46 mmol/g) was purchased from Pcas Biomatrix Inc. Sterile media [Dulbecco's modified Eagle medium (DMEM) L-glutamine, fetal bovine serum (FBS), and penicillin−streptomycin], fluorescent dyes (NHS-fluorescein, Mitotracker, Lysotracker, and Hoechst), and buffers [phosphate buffered saline (PBS)] used in cell culture were purchased from commercial sources. Melittin and amoxycillin were purchased from Sigma-Aldrich.

Synthesis of Compound 2. The synthesis of **2** proceeded as previously reported,[17] with the following minor modifications. To a solution of NaH (1.58 g, 65.9 mmol) in tetrahydrofuran (THF, 150 mL) with 4 Å mol sieves at 0 °C and under N_2 atmosphere was added an ice-cooled solution of **1** (5.0 g, 18.8 mmol) in THF (50 mL). The mixture was stirred at 0 °C for 1 h. To this mixture was added acrylonitrile (5.0 mL, 93.4 mmol), and the reaction was allowed to warm to room temperature and stirred for 24 h. The reaction mixture was cooled to 0 °C, and water (100 mL) was added to quench the excess NaH. The THF was removed *in vacuo*, and HCl (10%) was added to bring the solution to a pH of 1. The resulting solution was extracted with EtOAc (3×), the organic layers were dried over anhydrous $MgSO_4$, and the solvent was removed *in vacuo*. The desired product was purified by silica gel column chromatography [95% dichloromethane (DCM), 4% MeOH, 1% AcOH] to provide **2** as a colorless oil in 80% yield. Characterization of **2** was previously reported.[17]

Synthesis of Compound 3. To a solution of **2** (600 mg, 1.9 mmol) in 20 mL of ethanol was added 10% Pd/C (60 mg). The solution was stirred under 1 atm of hydrogen for 3 h. The solution was gravity filtered through filter paper, the solvent was removed *in vacuo*, and the resulting material was used in the next step without further purification. The material from the previous step was dissolved in deionized water (10 mL), the solution was cooled to 0 °C, and sodium bicarbonate (475 mg, 5.7 mmol) was added. To this cooled mixture, a solution of Fmoc-OSu (699 mg, 2.1 mmol) in 10 mL of acetone was added dropwise, and the resulting slurry was allowed to warm to room temperature and stirred overnight. The reaction mixture was treated with 10% HCl to a pH of 1 and extracted with EtOAc (3×). The organic layers were dried over anhydrous Na_2SO_4, and the solvent was removed *in vacuo*. The desired product was purified by silica gel column chromatography (96% DCM, 3% MeOH, 1% AcOH) to provide **3** as a white solid in quantitative yield. ^{1}H NMR (400 MHz, $CDCl_3$): δ10.14 (br s, 1H), 7.73 (dd, J = 24 Hz, 8

https://dx.doi.org/10.1021/acs.joc.0c00871
J. Org. Chem. 2020, 85, 7468−7475

Hz, 2H), 7.55 (m, 2H), 7.34 (m, 4H), 4.40−4.51 (m, 3H), 4.24−4.36 (m, 1H), 4.13 (m, 1H), 3.51−3.75 (m, 4H), 2.55 (q, J = 8 Hz, 2H), 2.33−2.48 (m, 1H), 2.11−2.26 (m, 1H). ^{13}C NMR (100 MHz, $CDCl_3$): δ 177.2*, 175.6, 155.7, 154.5*, 143.6, 141.2, 129.0, 127.7, 127.0, 124.9, 119.9, 117.4, 67.9, 63.7, 57.9, 57.2*, 51.4, 47.0, 36.6*, 34.7, 19.0 (*indicates minor rotamer). HRMS (APCI): calcd for $C_{23}H_{22}N_2O_5$ [M + H$^+$], 407.1601 m/z; found, 407.1598.

Synthesis of P_R.[17] To a solution of **3** (700 mg, 1.7 mmol) in 20 mL of MeOH was added 1 mL of AcOH, followed by PtO_2 (70 mg). The solution was stirred under 1 atm of hydrogen overnight. The solution was filtered through celite, the solvent was removed *in vacuo*, and toluene was used to remove excess AcOH. The resulting material was used in the next step without further purification. The material from the previous step was dissolved in 15 mL DCM and cooled to 0 °C. To this cooled mixture, a solution of triethylamine (0.720 mL, 5.2 mmol) in 5 mL DCM was added dropwise, followed by *N*,*N*′-bis-Boc-1-guanylpyrazole (695 mg, 2.2 mmol). The resulting slurry was allowed to warm to room temperature and stirred overnight. The reaction was extracted with DCM (3×), the organic layers were dried over anhydrous Na_2SO_4, and the solvent was removed *in vacuo*. The desired product was purified by silica gel column chromatography (96% DCM, 3% MeOH, 1% AcOH) to provide $\mathbf{P_R}$ as a white solid in 62% yield. Characterization of $\mathbf{P_R}$ was previously reported.[17]

Peptide Synthesis. H-Rink Chem Matrix Rink amide resin (200 mg, 0.46 mmol/g, 100−200 mesh) was added to a 10 mL peptide synthesis flask and washed with DMF, CH_2Cl_2, MeOH, and CH_2Cl_2 (7 mL, 2× each). The resin was swelled by adding DMF (7 mL) to the flask, and the flask was agitating for 30 min. After 30 min, the DMF was drained, and the resin was washed with DMF, CH_2Cl_2, MeOH, and CH_2Cl_2 (7 mL, 2× each). Following this wash, Fmoc-protected amino acids [(Fmoc-P_R (2 equiv), Fmoc-P_L (2 equiv), Fmoc-Lys-Mtt (4 equiv), or Fmoc-gly (4 equiv)] were dissolved in 7 mL of DMF, and HATU (2 or 4 equiv) and DIEA (4 or 8 equiv) were added. This amino acid solution was added to the peptide flask and agitated for 3 h at room temperature. After 3 h, the solution was drained, and the resin was washed with DMF, CH_2Cl_2, MeOH, and CH_2Cl_2 (7 mL, 2× each). To deprotect the amino acid, a piperidine (7 mL, 25% in DMF) solution was added to the flask and agitated for 25 min. The piperidine solution was drained and washed with DMF, CH_2Cl_2, MeOH, and CH_2Cl_2 (7 mL, 2× each). This procedure was repeated for each sequential amino acid in the peptide sequence. The Fmoc-protecting group of the final amino acid was deprotected with piperidine (7 mL, 25% in DMF). The N-terminus of CAPHs was functionalized by adding a DMF (7 mL) solution of carboxylic acid [featuring one of the hydrophobic groups (4 equiv)], HATU (4 equiv), and DIEA (8 equiv) to the peptide flask and agitating for 3 h. Successful amino acid couplings/deprotections were monitored via Kaiser (1° amino acid) or Chloranil (2° amino acid) tests.[29,30]

Deprotection of MTT Side Chain, Coupling of Fluorescein. Following coupling of the hydrophobic group to the N-terminus, the above resin was washed with CH_2Cl_2, MeOH, and CH_2Cl_2 (7 mL, 2× each). For each N-terminus hydrophobic modification, an aliquot of resin (∼50 mg) was transferred to a separate 10 mL synthesis flask. The resin was treated with HFIP (7 mL, 30% in DCM) and agitated for 30 min. This procedure was repeated twice, and the resin was washed with CH_2Cl_2, MeOH, and CH_2Cl_2 (7 mL, 2× each) after each HFIP wash. Successful Mtt deprotection was monitored by the Kaiser test. The resin was washed with DMF, CH_2Cl_2, MeOH, and CH_2Cl_2 (7 mL, 2× each), and N-hydroxysuccinimide fluorescein (1.2 equiv) and DIEA (2.4 equiv) in DMF (7 mL) was allowed to react with the resin for 16 h in the dark. The resin was then washed with CH_2Cl_2, MeOH, and CH_2Cl_2 (7 mL, 2× each).

Cleavage and Purification of Peptides. A fresh TFA cocktail solution of 10 mL (95% TFA, 2.5% TIPS, 2.5% H_2O) was prepared and was added to the resin and agitated for 2 h. After 2 h, the solution was drained into a 50 mL centrifuge tube. The resin was subsequently washed with the TFA cocktail (10 mL, 2×) and CH_2Cl_2 (10 mL, 2×), and all the filtrate was collected. TFA was removed *in vacuo*, and the peptide was precipitated with ice-cold diethyl ether (15 mL) overnight at −79 °C. The filtrate was centrifuged (3500 RPM, 15 min) and dried. The peptide was purified to homogeneity (>95% pure, Figure S1) using RP-HPLC using a gradient of 25−80% of CH_3CN (0.1% TFA) in water (0.1% TFA). The gradient was run for 60 min using a Luna C18 semi-prep column, using a flow rate of 10.0 mL/min and monitored with a UV detector at 214 and 254 nm. The mass of the peptides was confirmed via MALDI-time of flight (MALDI-TOF) mass spectrometry, and the concentration of aqueous stock solutions of peptides were confirmed using UV−visible spectroscopy at a wavelength of 518 nm.

Circular Dichroism. Data were recorded on a Jasco CD spectropolarimeter (Model J-1500) at 25 °C using a 1 mm path length quartz cell. The spectra were averaged over three scans taken from 260 to 190 nm, with a data pitch and bandwidth of 1 nm, at a scan rate of 20 nm/min. All peptides were analyzed at 50 μM concentration in 20 mM phosphate buffer (pH 7.2). The spectra were background-subtracted and processed from degrees of rotation to mean residue ellipticity by dividing by the appropriate path length, peptide concentration, and number of residues in the peptide.

Cell Uptake. J774A.1 cells were cultured in DMEM supplemented with 10% FBS, and 1% penicillin/streptomycin at 37 °C under 5% CO_2 atmosphere. J774A.1 cells (125,000) were harvested and transferred to round-bottom tubes (BD Biosciences) and allowed to adhere overnight. The next day, these cells were treated with CAPHs (2.5−10 μM) in 10% FBS-supplemented DMEM (300 μL) and were incubated for 1 h at 37 °C. Cells with no CAPHs treatment (DMEM supplemented with 10% FBS only) served as a control for the experiment. Upon completion of the 1 h incubation period, the cells were centrifuged (1100 rpm, 7 min @ 4 °C), and the spent media was aspirated. The cells were resuspended in TB (400 μL, 1 mg/mL in PBS), and the fluorescence of the cells was measured using a FACSCalibur Flow Cytometer (BD Biosciences) equipped with a 488 nm argon laser. Emissions for fluorescein-labeled peptides were collected in the FL 1 channel. Data were obtained in duplicate from three independent experiments and processed using the BD software.

Cell Toxicity. The viability of J774A.1 cells with CAPHs peptides was determined via a colorimetric MTT assay. In Brief, J774A.1 cells (20,000) were cultured at 37 °C under 5% CO_2 atmosphere and were seeded into a sterile 96-well plate and allowed to adhere for 24 h. The spent media was aspirated, and the J774A.1 cells were treated with CAPHs (10 μM in DMEM supplemented with 10% FBS) for 9 h at 37 °C. After this incubation period, the treatment was aspirated, and the cells were washed with PBS. Next, 100 μL of fresh DMEM media was added to each well, followed by 10 μL of 12 mM MTT reagent. The plate was incubated for an additional 2 h at 37 °C under 5% CO_2 atmosphere. Finally, the MTT solution was aspirated, and 100 μL of DMSO was added to each well. The 96-well plate was allowed to shake for 5 min at room temperature, and the absorbance of each well was measured at 590 nm using a microplate reader. Results were expressed as the percentage of viable cells as compared to a control that contained no CAPHs treatment. Data were obtained in duplicate from three independent experiments.

Subcellular Localization. J774A.1 cells (200,000) were seeded in a 4-well Lab-Tek chambered slide and were allowed to adhere for 18 h at 37 °C under 5% CO_2 atmosphere. The media was then aspirated, and the cells were washed with PBS (400 μL). Next, CAPHs were added to each well in 400 μL of DMEM supplemented with 10% FBS. The cells were incubated for 1 h at 37 °C under 5% CO_2 atmosphere. After the incubation period, the treatment was aspirated and washed with PBS (400 μL). The cells were further treated with Hoechst 33342 (1000 nM) and either Mitotracker (100 nM) or Lysotracker (300 nM) for 30 min at 37 °C under 5% CO_2 atmosphere. The excess dye was aspirated, the cells were washed with 400 μL of PBS, and fresh serum-supplemented DMEM was added to each well. Imaging was performed using a Nikon A1R multiphoton inverted confocal microscope under a 60× oil objective. Fluorescein, Hoechst 33342, and Mitotracker/Lysotracker were excited using 488, 350, and 561 nm lasers, respectively.

***β*-Galactosidase Assay.** *E. coli* (ATCC 25922) was grown to the mid-exponential phase (OD_{590} = ∼0.6) in Mueller−Hinton Broth (MHB) at 37 °C with shaking. *β*-Galactosidase expression was

https://dx.doi.org/10.1021/acs.joc.0c00871
J. Org. Chem. 2020, 85, 7468−7475

induced for 1 h using a freshly prepared solution of isopropyl-β-D-thiogalactopyranoside in PBS (1 mM final concentration). Following the induction, an aliquot (10 mL) of the bacterial suspension was centrifuged, washed twice with fresh MHB, and plated into a sterile 96-well plate. Next, 10 μL aliquots of CAPHs were added to give final concentrations corresponding to 1×, 2×, or 4× the MIC value (against *E. coli*). Bacteria were also treated with sterile water and melittin (20 μM final concentration), which served as controls. The 96-well plate was incubated for 1 h at 37 °C. At the end of the incubation period, the plate was centrifuged at 4000 rpm for 10 min. A volume of 80 μL of the supernatant from each well as added to a new sterile 96-well plate. Next, 20 μL of freshly prepared 2-nitrophenyl-β-D-galactopyranoside in PBS was added to each well (0.8 mg/mL final concentration). The β-galactosidase activity was monitored at OD_{405nm} every 5 min over the course of 1 h using a microplate reader. Data were obtained in duplicate from at least two independent experiments.

Hemolysis. hRBCs were centrifuged at 1200 rpm at 4 °C for 5 min. The hRBCs were washed with PBS (pH 7.4) two times, and a 4% suspension (v/v) of hRBCs was prepared in PBS. A volume of 50 μL of the hRBCs solution was transferred to a sterile 96-well plate, and 50 μL of CAPHs in PBS was added to each well to give a final suspension of 2% (v/v) of hRBCs. The plate was then incubated for 1 h at 37 °C. At the end of the incubation, the plate was centrifuged at 1200 rpm for 5 min at 4 °C. From each well, 80 μL of the supernatant was then transferred to a new sterile 96-well plate. Finally, the release of hemoglobin caused by hemolysis was quantified by measuring the absorbance of the wells at 405 nm with a microplate reader. For controls, wells were treated with PBS, melittin, or 0.1% (final concentration) Triton X-100 in PBS. The percentage of hemolysis was calculated on the basis of the 100% hemolysis release with 0.1% Triton X-100. Data were obtained in duplicate from at least two independent experiments.

Antimicrobial Susceptibility Testing. The antimicrobial activity of the CAPHs and control antibiotics against the tested isolates, except for *M. tuberculosis*, was performed following the Clinical and Laboratory Standards Institute guidelines.[31] Briefly, bacterial cells were cultured overnight on trypticase soya agar plates (Becton Dickinson). Colonies were picked and suspended in NaCl 0.9% to a density of 0.5 McFarland. The bacterial suspensions were further diluted 1:60 in CA-MHB (cation adjusted Mueller−Hinton Broth Becton Dickinson), and 100 μl portions of the bacterial suspension were added to 96-well plates containing the CAPHs and control antibiotics at a concentration range of 0.125−16 μM. The 96-well plates were incubated for 16−20 h at 37 °C before recording the MIC values. The MICs reported represent the lowest concentration of each peptide or standard antibiotic necessary to inhibit the bacterial growth. For testing the antimicrobial activity of the CAPHs and control antibiotic against *M. tuberculosis*, a resazurin microtiter assay was performed following a previously reported protocol.[32] Briefly, mycobacterial colonies grown on the Lowenstein−Jensen (Becton Dickinson) medium were suspended in the 7H9-S broth, adjusted spectrophotometrically to a no. 1 McFarland tube standard, and further diluted 1:10 in 7H9-S broth. Then, 100 μl of the 7H9-S broth was dispensed in each well of a sterile flat-bottom 96-well plate, and serial twofold dilutions of each of the peptides and control antibiotics were prepared directly in the plate. One-hundred microliters of the prepared inoculum was added to each well. Plates were covered, sealed in a plastic bag, and incubated at 37 °C under a normal atmosphere. After 7 days of incubation, 30 μL of resazurin solution, 0.02% (w/v) in distilled water, was added to each well, and the plate was re-incubated overnight. A change in color from blue to pink indicated the growth of bacteria, and the MIC was defined as the lowest concentration of the compound that prevented this change in color.

Activity against Intracellular Bacteria. Following previously described protocols, the ability of the peptides to reduce the burden of intracellular *S. flexneri* was evaluated.[16,33] Murine macrophage cells (J774A.1) were cultured in DMEM supplemented with 10% FBS at 37 °C under a CO_2 (5%) atmosphere. J774.1 cells were infected with *S. flexneri* 1a ATCC 9199 cells at a multiplicity of infection of approximately 1:100. After 1 h of infection, J774A.1 cells were washed with DMEM and further incubated with gentamicin (100 μg/mL) for 1 h to kill extracellular bacteria. The peptides at the respective concentrations were added to each well (four replicates per test agent). After 12 h incubation at 37 °C with 5% CO_2, the compounds were removed, J774A.1 cells were washed and lysed using 0.1% Triton-X. The cell lysates were serially diluted in PBS and transferred to trypticase soy agar plates to determine viable bacterial cfu, inside the J774A.1 cells. The plates were incubated at 37 °C for 20 h before counting viable cfu/mL. Data are presented as the percentage of intracellular cfu/mL in treated murine macrophage cells relative to the untreated control.

■ ASSOCIATED CONTENT

Supporting Information

The Supporting Information is available free of charge at https://pubs.acs.org/doi/10.1021/acs.joc.0c00871.

Mass spectrometry data, RP-HPLC retention times and traces, and CD spectra of N-terminal CAPHs; cell viability test data; β-galactosidase assay data; Cellular uptake of aliphatic N-terminal CAPHs in J774A.1 macrophage cells; and cell localization data (PDF)

■ AUTHOR INFORMATION

Corresponding Author

Jean Chmielewski − *Department of Chemistry, Purdue University, West Lafayette, Indiana 47907-2027, United States;* orcid.org/0000-0003-4958-7175; Email: chml@purdue.edu

Authors

Thomas A. Dietsche − *Department of Chemistry, Purdue University, West Lafayette, Indiana 47907-2027, United States*

Hassan E. Eldesouky − *Department of Comparative Pathobiology, Purdue University, West Lafayette, Indiana 47907-2027, United States;* orcid.org/0000-0003-4718-6087

Samantha M. Zeiders − *Department of Chemistry, Purdue University, West Lafayette, Indiana 47907-2027, United States*

Mohamed N. Seleem − *Department of Comparative Pathobiology, Purdue University, West Lafayette, Indiana 47907-2027, United States;* orcid.org/0000-0003-0939-0458

Complete contact information is available at: https://pubs.acs.org/10.1021/acs.joc.0c00871

Author Contributions

The manuscript was written through contributions of all authors.

Notes

The authors declare no competing financial interest.

■ ACKNOWLEDGMENTS

The authors acknowledge support from the National Science Foundation (1609406-CHE).

■ REFERENCES

(1) Kumarasamy, K. K.; Toleman, M. A.; Walsh, T. R.; Bagaria, J.; Butt, F.; Balakrishnan, R.; Chaudhary, U.; Doumith, M.; Giske, C. G.; Irfan, S.; Krishnan, P.; Kumar, A. V.; Maharjan, S.; Mushtaq, S.; Noorie, T.; Paterson, D. L.; Pearson, A.; Perry, C.; Pike, R.; Rao, B.; Ray, U.; Sarma, J. B.; Sharma, M.; Sheridan, E.; Thirunarayan, M. A.; Turton, J.; Upadhyay, S.; Warner, M.; Welfare, W.; Livermore, D. M.;

Woodford, N. Emergence of a New Antibiotic Resistance Mechanism in India, Pakistan, and the UK: A Molecular, Biological, and Epidemiological Study. *Lancet Infect. Dis.* **2010**, *10*, 597−602.
(2) Navon-Venezia, S.; Ben-Ami, R.; Carmeli, Y. Update on Pseudomonas aeruginosa and Acinetobacter baumannii infections in the healthcare setting. *Curr. Opin. Infect. Dis.* **2005**, *18*, 306−313.
(3) Smith, I. Mycobacterium tuberculosis Pathogenesis and Molecular Determinants of Virulence. *Clin. Microbiol. Rev.* **2003**, *16*, 463−496.
(4) Flannagan, R. S.; Cosío, G.; Grinstein, S. Antimicrobial Mechanisms of Phagocytes and Bacterial Evasion Strategies. *Nat. Rev. Microbiol.* **2009**, *7*, 355−366.
(5) Diacovich, L.; Gorvel, J.-P. Bacterial Manipulation of Innate Immunity to Promote Infection. *Nat. Rev. Microbiol.* **2010**, *8*, 117−128.
(6) Carryn, S.; Chanteux, H.; Seral, C.; Mingeot-Leclercq, M.-P.; Van Bambeke, F.; Tulkens, P. M. Intracellular Pharmacodynamics of Antibiotics. *Infect. Dis. Clin.* **2003**, *17*, 615−634.
(7) Seleem, M. N.; Munusamy, P.; Ranjan, A.; Alqublan, H.; Pickrell, G.; Sriranganathan, N. Silica-Antibiotic Hybrid Nanoparticles for Targeting Intracellular Pathogens. *Antimicrob. Agents Chemother.* **2009**, *53*, 4270−4274.
(8) Kalluru, R.; Fenaroli, F.; Westmoreland, D.; Ulanova, L.; Maleki, A.; Roos, N.; Paulsen Madsen, M.; Koster, G.; Egge-Jacobsen, W.; Wilson, S.; Roberg-Larsen, H.; Khuller, G. K.; Singh, A.; Nystrom, B.; Griffiths, G. Poly(Lactide-Co-Glycolide)-Rifampicin Nanoparticles Efficiently Clear Mycobacterium Bovis BCG Infection in Macrophages and Remain Membrane-Bound in Phago-Lysosomes. *J. Cell Sci.* **2013**, *126*, 3043−3054.
(9) Lei, E. K.; Pereira, M. P.; Kelley, S. O. Tuning the Intracellular Bacterial Targeting of Peptidic Vectors. *Angew. Chem., Int. Ed.* **2013**, *52*, 9660−9663.
(10) Ahmed, M.; Kelley, S. O. Enhancing the Potency of Nalidixic Acid toward a Bacterial DNA Gyrase with Conjugated Peptides. *ACS Chem. Biol.* **2017**, *12*, 2563−2569.
(11) Alajlouni, R. A.; Seleem, M. N. Targeting Listeria Monocytogenes RpoA and RpoD Genes Using Peptide Nucleic Acids. *Nucleic Acid Ther.* **2013**, *23*, 363−367.
(12) Brezden, A.; Mohamed, M. F.; Nepal, M.; Harwood, J. S.; Kuriakose, J.; Seleem, M. N.; Chmielewski, J. Dual Targeting of Intracellular Pathogenic Bacteria with a Cleavable Conjugate of Kanamycin and an Antibacterial Cell-Penetrating Peptide. *J. Am. Chem. Soc.* **2016**, *138*, 10945−10949.
(13) Kuriakose, J.; Hernandez-Gordillo, V.; Nepal, M.; Brezden, A.; Pozzi, V.; Seleem, M. N.; Chmielewski, J. Targeting Intracellular Pathogenic Bacteria with Unnatural Proline-Rich Peptides: Coupling Antibacterial Activity with Macrophage Penetration. *Angew. Chem., Int. Ed.* **2013**, *52*, 9664−9667.
(14) Nepal, M.; Thangamani, S.; Seleem, M. N.; Chmielewski, J. Targeting Intracellular Bacteria with an Extended Cationic Amphiphilic Polyproline Helix. *Org. Biomol. Chem.* **2015**, *13*, 5930−5936.
(15) Lee, J. S.; Tung, C.-H. Lipo-Oligoarginines as Effective Delivery Vectors to Promote Cellular Uptake. *Mol. BioSyst.* **2010**, *6*, 2049.
(16) Nepal, M.; Mohamed, M. F.; Blade, R.; Eldesouky, H. E.; N Anderson, T.; Seleem, M. N.; Chmielewski, J. A Library Approach to Cationic Amphiphilic Polyproline Helices That Target Intracellular Pathogenic Bacteria. *ACS Infect. Dis.* **2018**, *4*, 1300−1305.
(17) Fillon, Y. A.; Anderson, J. P.; Chmielewski, J. Cell Penetrating Agents Based on a Polyproline Helix Scaffold. *J. Am. Chem. Soc.* **2005**, *127*, 11798−11803.
(18) Tseng, W.-H.; Li, M.-C.; Horng, J.-C.; Wang, S.-K. Strategy and Effects of Polyproline Peptide Stapling by Copper(I)-Catalyzed Alkyne−Azide Cycloaddition Reaction. *ChemBioChem* **2019**, *20*, 153−158.
(19) Helbecque, N.; Loucheux-Lefebvre, M. H. Critical Chain Length for Polyproline-II Structure Formation in H-Gly-(Pro)n-OH. *Int. J. Pept. Protein Res.* **1982**, *19*, 94−101.
(20) Bjerknes, R.; Bassøe, C.-F. Phagocyte C3-Mediated Attachment and Internalization: Flow Cytometric Studies Using a Fluorescence Quenching Technique. *Blut* **1984**, *49*, 315−323.
(21) Kalafut, D.; Anderson, T. N.; Chmielewski, J. Mitochondrial Targeting of a Cationic Amphiphilic Polyproline Helix. *Bioorganic Med. Chem. Lett.* **2012**, *22*, 561−563.
(22) Riss, T. L.; Moravec, R. A.; Niles, A. L.; Benink, H. A.; Worzella, T. J. Cell Viability Assays. *Assay Guidance Manual*; Eli Lilly & Company and the National Center for Advancing Translational Sciences, 2016; pp 1−31.
(23) Pereira, M. P.; Shi, J.; Kelley, S. O. Peptide Targeting of an Antibiotic Prodrug toward Phagosome-Entrapped Mycobacteria. *ACS Infect. Dis.* **2015**, *1*, 586−592.
(24) Bai, H.; You, Y.; Yan, H.; Meng, J.; Xue, X.; Hou, Z.; Zhou, Y.; Ma, X.; Sang, G.; Luo, X. Antisense Inhibition of Gene Expression and Growth in Gram-Negative Bacteria by Cell-Penetrating Peptide Conjugates of Peptide Nucleic Acids Targeted to RpoD Gene. *Biomaterials* **2012**, *33*, 659−667.
(25) Howard, A.; Donoghue, M. O.; Feeney, A.; Sleator, R. D. Acinetobacter Baumannii an Emerging Opportunistic Pathogen. *Virulence* **2012**, *3*, 243−250.
(26) Porter, E. A.; Weisblum, B.; Gellman, S. H. Mimicry of Host-Defense Peptides by Unnatural Oligomers: Antimicrobial β-Peptides. *J. Am. Chem. Soc.* **2002**, *124*, 7324−7330.
(27) Seleem, M. N.; Jain, N.; Pothayee, N.; Ranjan, A.; Riffle, J. S.; Sriranganathan, N. Targeting Brucella Melitensis with Polymeric Nanoparticles Containing Streptomycin and Doxycycline. *FEMS Microbiol. Lett.* **2009**, *294*, 24−31.
(28) Li, L.; Geisler, I.; Chmielewski, J.; Cheng, J.-X. Cationic Amphiphilic Polyproline Helix P11LRR Targets Intracellular Mitochondria. *J. Control. Release* **2010**, *142*, 259−266.
(29) Christensen, T.; Eriksson, A.; Thornell, L.-E. Qualitative Test for Monitoring Coupling Completeness in Solid-Phase Peptide-Synthesis Using Chloranil. *Acta Chem. Scand., Ser. B* **1979**, *33*, 763−766.
(30) Kaiser, E.; Colescott, R. L.; Bossinger, C. D.; Cook, P. I. Color Test for Detection of Free Terminal Amino Groups in the Solid-Phase Synthesis of Peptides. *Anal. Biochem.* **1970**, *34*, 595.
(31) Clinical and Laboratory Standards Institute (CLSI); Weinstein, M. P.; Zimmer, B. L.; Cockerill, F. R.; Wiker, M. A.; Alder, J.; Dudley, M. N.; Eliopoulos, G. M.; Ferraro, M. J.; Hardy, D. J.; Hecht, D. W.; Hindler, J. A.; Patel, J. B.; Powell, M.; Swenson, J. M.; Thomson, R. B.; Traczewski, M. M.; Turnidge, J. D. *Methods for Dilution Antimicrobial Susceptibility Tests for Bacteria that Grow Aerobically*; Approved Standard, 9th ed., 2012; Vol. *32*.
(32) Martin, A.; Camacho, M.; Portaels, F.; Palomino, J. C. Resazurin microtiter assay plate testing of Mycobacterium tuberculosis susceptibilities to second-line drugs: rapid, simple, and inexpensive method. *Antimicrob. Agents Chemother.* **2003**, *47*, 3616−3619.
(33) Chiu, H.-C.; Kulp, S. K.; Soni, S.; Wang, D.; Gunn, J. S.; Schlesinger, L. S.; Chen, C.-S. Eradication of Intracellular Salmonella Enterica Serovar Typhimurium with a Small-Molecule, Host Cell-Directed Agent. *Antimicrob. Agents Chemother.* **2009**, *53*, 5236−5244.

https://dx.doi.org/10.1021/acs.joc.0c00871
J. Org. Chem. 2020, 85, 7468−7475